International Journal of Solids and Structures 48 (2011) 603–610

Contents lists available at ScienceDirect

International Journal of Solids and Structures

journal homepage: www.elsevier.com/locate/ijsolstr

An exponential law for stretching–relaxation properties of bone piezovoltages

Zhende Hou [a,*], Donghui Fu [a], Qing-Hua Qin [b]

[a] Department of Mechanics, School of Mechanical Engineering, Tianjin University, Tianjin 300072, China
[b] School of Engineering, Australian National University, Canberra, ACT 0200, Australia

ARTICLE INFO

Article history:
Received 23 February 2010
Received in revised form 15 October 2010
Available online 25 October 2010

Keywords:
Piezoelectricity
Bone
Piezovoltage
Relaxation
Stretched exponentials

ABSTRACT

An exponential law is presented for modeling piezoelectric behavior of bone tissues. The law is established based on experimental observation and existing empirical decay function. The model is then used to investigate the relaxation behavior of pizeovoltages induced by external load. Piezovoltages between the two opposing surfaces of bovine tibia bone samples under three point bending deformation are measured using an ultra high input impedance bioamplifier. The experimental results indicate that the pizeovoltages of bone show different relaxation behaviors during loading and unloading process. It is found that the piezovoltage decay follows a stretched exponential law when the load increases from zero to its maximum value, while it follows a typical relaxation exponential law when the load is kept its maximum value. The stretching-exponential behavior is independent of loading amplitude and rate. One possible reason for causing the stretched exponential behavior may be due to the triple helices structure of collagen fibrils distributed randomly in bone, which can experience relatively large deformation under external loads. The deformation process may include self-deformation and relative slipping between the molecule chains. The relative slipping movements may change the dielectric constants and resistances of bone, which can lead to multiple relaxation time behaviors during the deformation process of bone.

1. Introduction

Bone can change its mass, shape and density to adapt its external environment, which is called bone remodeling, the substance of Wolf law. There are generally three possible factors to influence the bone remodeling process. They are piezoelectric potential (Fukada, 1964; Bassett and Becker, 1962; Steinberg et al., 1968; Qin and Ye, 2004; Qin et al., 2005) and streaming potentials (Anderson and Eriksson, 1968; Yokota and Tanaka, 2005; Pienkowski and Pollack, 1983) both of which are known as stress generated potentials (SGPs). The third one is fluid-generated shear stress (Tzima et al., 2005; Burger et al., 2003; Riddle and Donahue, 2008). From the viewpoint of biologic evolution, though whether the electric potential of bone has any effect on remodeling is still an open question, bone's mechanical–electrical coupling property may have effects on the bone remodeling process in some way. Thus, the piezoelectricity of bone may play a certain role in bone remodeling process.

In the literature, piezoelectric signals were usually measured by charge amplifier, which detected the polarized charges on bone surfaces by transferring them to a capacitor in an instrument. This is a relatively simple way for determining the quantitative relationships between the electric charge and external force. However, this method cannot reveal the time-dependent variation of the polarized charges in bone during which the magnitude of charges may influence the bone remodeling process or osteocyte viability.

During the past decades, various new techniques have been developed and employed to investigate the piezoelectric properties of bone tissue. Based on the concept of converse piezoelectric effect (Qin, 2001), the piezoelectric coefficient d_{23} was determined using a sensitive dilatometer (Aschero et al., 1999). Piezoelectric force microscope and atomic force microscope were also employed to measure piezoelectric properties of bone (Kalinin et al., 2005; Minary-Jolandan and Yu, 2009). As bone belongs to an inhomogeneous anisotropy material, the piezoelectric coefficient matrix at a point does not convey enough information of its piezoelectric properties. In order to investigate in detail the piezoelectric properties of bone, it is necessary to conduct further studies with different methods. In this study, the piezovoltage of bone under three-point bending deformation are measured using an ultra high input impedance bioamplifier. The pizeovoltage of bone show different stretching–relaxation behaviors during loading and unloading process. It also follows different exponential law during stretching and relaxation process.

* Corresponding author. Tel.: +86 22 27406719; fax: +86 22 27892213.
E-mail address: hou@tju.edu.cn (Z. Hou).

0020-7683/$ - see front matter © 2010 Elsevier Ltd. All rights reserved.
doi:10.1016/j.ijsolstr.2010.10.024

2. Materials and methods

2.1. Sample preparation

Cortical bone samples used are harvested from mid diaphysis of dry bovine tibias (age 2–3 years), and machined into rectangular beams (Fig. 1(a)) with a dimension range as shown in Table 1. Six samples were prepared and were dried in air for at least two weeks till the resistance or impedance between the two lateral surfaces was over 10^9 Ohm, while the maximum resistance of complete dry bone is usually in the order of 10^{10} Ohm (Singh and Saha, 1984; Tzukert et al., 1983). Then, the conductive silver adhesive (5001, SPI, USA) was painted on both sides of each specimen as electrodes whose dimensions are of 3×3 mm (Fig. 1(b)). After the electrodes being painted, the samples were kept in an environment with relative humidity 52–56% and temperature 22–25 °C. The two electrodes were placed in the same axial position and at the same mid-height from the neutral axes of the samples, where the bone samples are subjected to both normal stress and shear stress.

2.2. Experimental set-up

The pair of electrodes and the bone tissue sandwiched between them is equivalent to a capacitor and let C be its capacitance (Singh and Saha, 1984; Johnson et al., 1980). Once the piezoelectric charge Q induced by the load accumulates on the electrodes, a corresponding piezovoltage V ($V = CQ$) can be observed. Because the piezovoltage is a linear function of piezocharge, the variation of the voltage is consistent with that of the charge.

The experimental setup of the measurement system is illustrated in Fig. 2. It can be seen from Fig. 2 that the electrode on the lateral side facing medullary cavity (Fig. 1) was taken as zero potential (or reference potential). While the measured piezovoltage was input into a Bioamplifier (BMA-931, CWE Inc., USA) via an ultra high input impedance (over $10^{12}\ \Omega$) Head Stage (Super Z, CWE Inc., USA), whose input impedance is at least two orders higher than that of bone and is able to prevent the charges accumulated on the electrodes leaking through the head stage. In the measurement, the amplified voltage signals were recorded by a computer. Loads were applied using an Instron 1343 closed-loop servo-hydraulic machine controlled by 8800 Control Tower, and the loading signals in Control Tower were also input into the computer for recording.

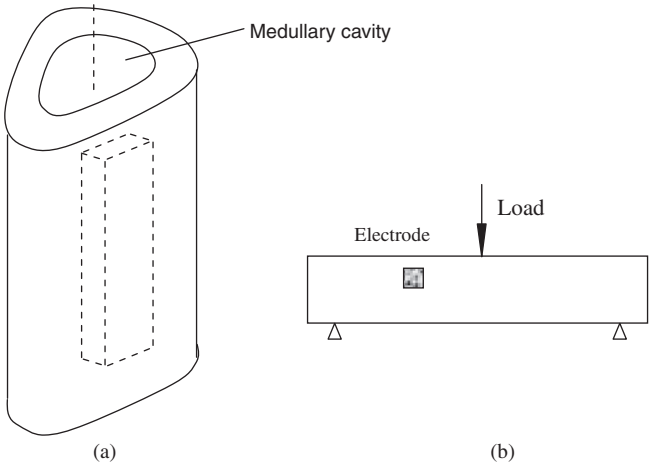

Fig. 1. (a) The geometry of the sample; (b) three-point test.

Table 1
Size of samples.

Span (mm)	Width (mm)	Height (mm)
85	4.0 ± 1.0	19 ± 3.0

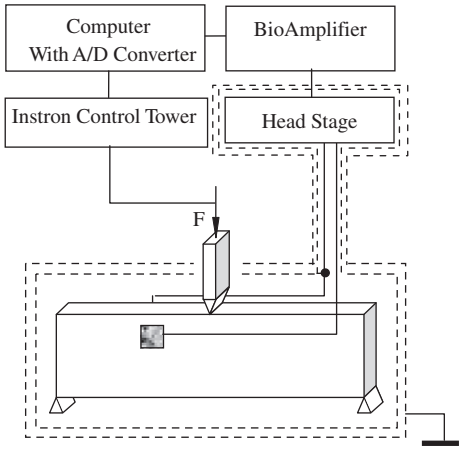

Fig. 2. Setup of the test system.

The testing sample and the Head Stage are enclosed in a double electromagnetic shield with the outer shield connecting to ground and the inner to the Head Stage common terminal. This arrangement can keep the electric field distribution to be constant in the device (Fu et al., 2006).

2.3. Experimental procedure and characteristic of piezovoltage

Fig. 3 shows a trapezoidal loading configuration applying to the samples in our experiment. It has equal loading and unloading time T_o (T_o = 0.25, 0.5 and 1 s is employed). Having reached its maximum F_o (F_o = 50, 100 and 150 N in our experiment), the load is kept to be constant for 6 s and then the load decreases to zero (see Fig. 3). It is noted that the cortical bone has a weak viscoelasticity especially dry bone (Yamashita et al., 2002). In order to reduce the effect of viscoelasticity, the maximum compressive stresses in the samples, caused by the maximum F_o, are between 12 and 23 MPa which is much less than 80 MPa below which no irrecoverable deformation occurs in cortical bone (Fondrk et al., 1988) and the stress and strain has a linear relationship for cortical bovine (Hoc et al., 2006).

Piezovoltages of the bone samples are measured under three-point bending in an environment with relative humidity of 52–56% and temperature of 21–26 °C. Fig. 3(b) shows a typical plot of variation of piezovoltage with time under the loading profile shown in Fig. 3(a). It has a negative and a positive pulse corresponding to the loading and unloading durations respectively. The peak of first pulse (negative) is just corresponding to the loading endpoint and the second pulse peak corresponds to the unloading endpoint. The amplitudes of the peaks are of the order of several millivolts. The pattern of the pulses indicates that once the loading or unloading ends the piezovoltage starts to decay towards zero, which looks like an exponential relaxation process. The corresponding physical process is that once the piezocharge appears on the two electrodes, it begins to discharge through the impedance of the bone. Then, the variation of the piezocharge with time is associated with mechanical loads and physical properties of bone such as impedance.

3. Results

The piezovoltage–time curves (Blue)[1] of all the samples (Fig. 4) are similar in shape under three point bending. Figs. 4 and 5

[1] For interpretation of color in Figs. 3–5 and 7, the reader is referred to the web version of this article.

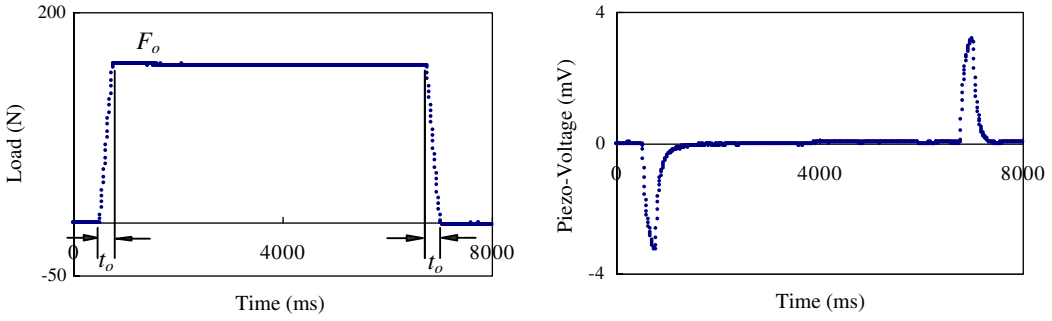

(a) Loading waveform (b) Piezovoltage waveform

Fig. 3. Loading and piezo-voltage wave form.

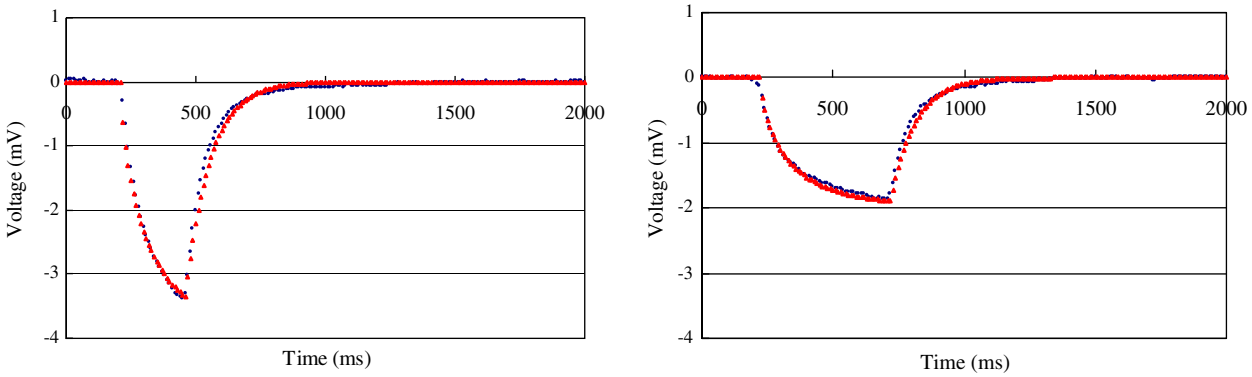

(a) Measured voltage and fitted curve at F_o=150 N and T_o=250 ms

(b) Measured voltage and fitted curve at F_o=150 N and T_o=500 ms

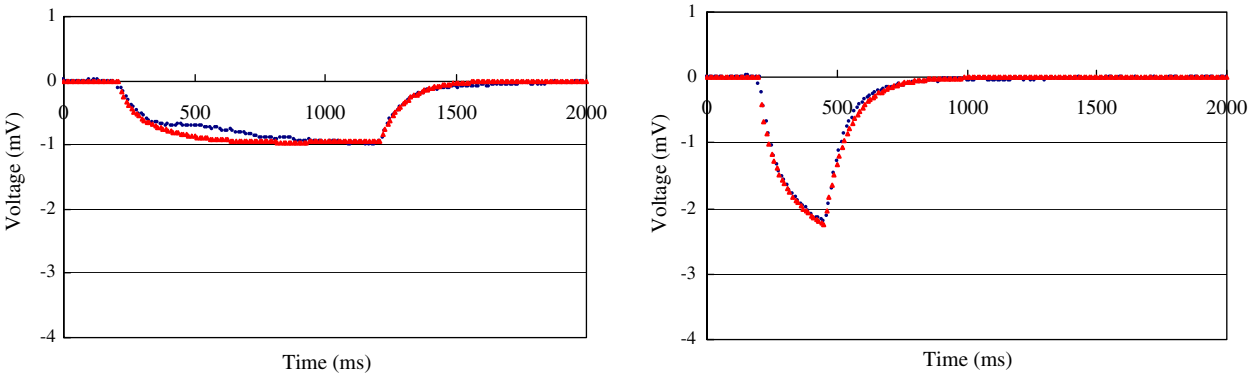

(c) Measured voltage and fitted curve at F_o=150 N and T_o=1000 ms

(d) Measured voltage and fitted curve at F_o=100 N and T_o=250 ms

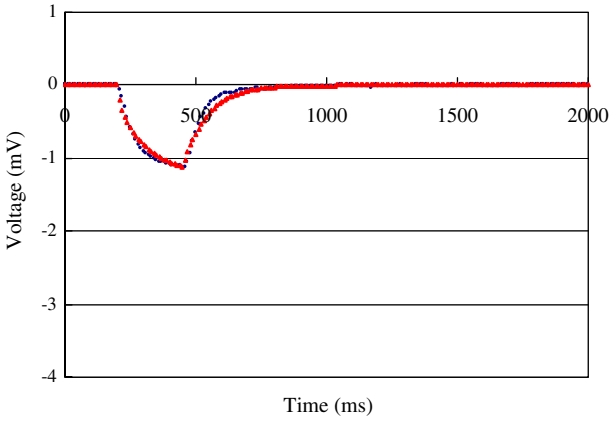

(e) Measured voltage and fitted curve at F_o=50 N and T_o=250 ms

Fig. 4. Fitting functions at different F_o and T_o for sample No. 1.

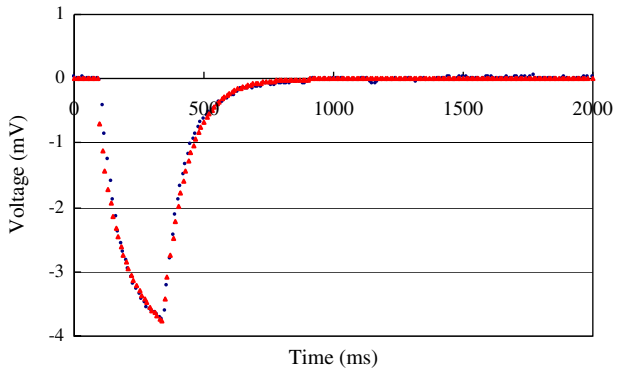

(a) Measured voltage and fitted curve at F_o=150 N and T_o=250 ms

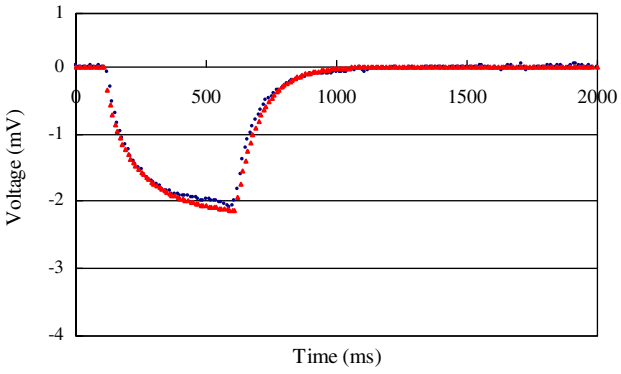

(b) Measured voltage and fitted curve at F_o=150 N and T_o=500

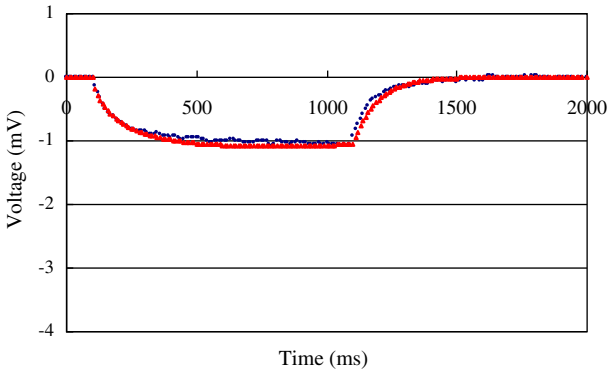

(c) Measured voltage and fitted curve at F_o=150 N and T_o=1000

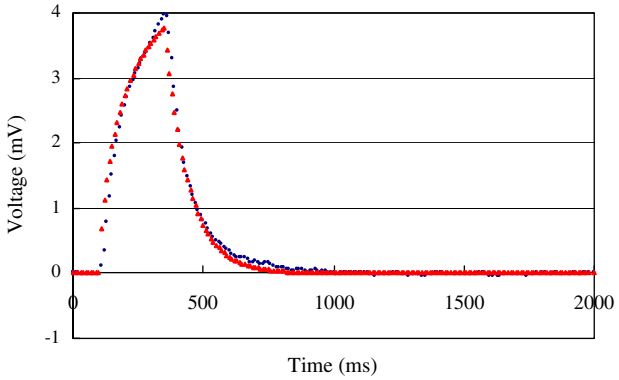

(d) Measured voltage and fitted curve at F_o=150 N and T_o=250 ms for unloading

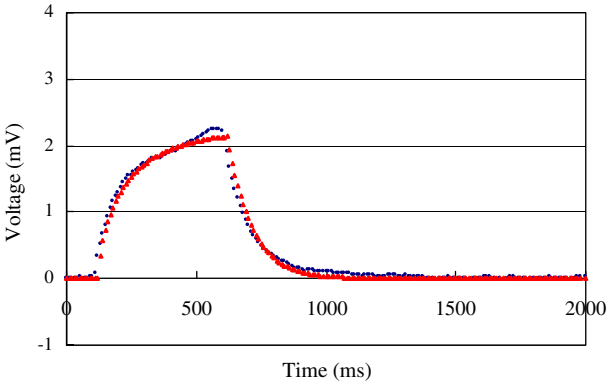

(e) Measured voltage and fitted curve at F_o=150 N and T_o=500 ms for unloading

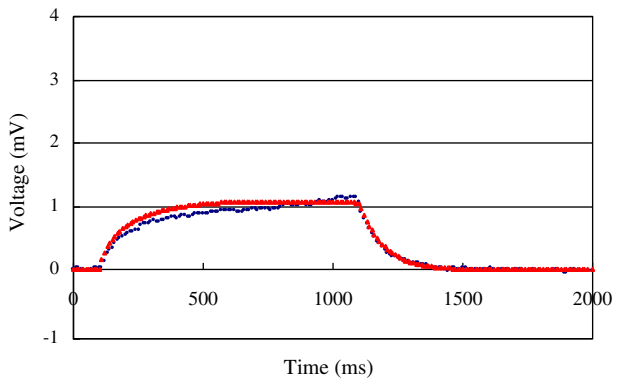

(f) T Measured voltage and fitted curve at F_o=150 N and T_o=1000 ms for unloading

Fig. 5. Fitting functions at different F_o and T_o for sample No. 2.

illustrate two groups of these curves for samples 1 and 2, respectively, with different loading conditions.

After many trials of curve fittings on the measured curves, it was found that the pizeovoltages show different relaxation behaviors in loading (or unloading) and load holding processes (details of fitting scheme can be found in Appendix A). During loading, the piezovoltage decays followed a non-exponential or stretched exponential law $e^{-(t/\tau_d)^{\beta}}$ (Williams and Watts, 1970), while they follows a typical exponential law ($\beta = 1$, known as Debye exponential relaxation) in the load holding duration. Eq. (1) below represents the fitting function for the measured piezovoltage $V(t)$,

$$V(t) = KF(t)e^{-\left(\frac{t}{\tau_d}\right)^{\beta}} \tag{1}$$

where t is the time, $F(t)$ the load function, K a proportional coefficient between load $F(t)$ and piezovoltage, τ_d is time constant or relaxation time, and β ($0 < \beta \leqslant 1$) is a stretching exponent. In our experiment, the first stage of the loading process $F(t)$ is given as

$$F(t) = F_0 \frac{t}{T_0} \quad (t \leqslant T_o) \tag{1'}$$

Eq. (1) indicates that the piezovoltage is generated in proportion to the load $F(t)$, and it decays in the stretched exponential law simultaneously.

When the loading keeps constant, the fitted piezovoltage function is

$$V(t) = V_o e^{-\frac{t}{\tau_c}} \tag{2}$$

where τ_c is a time constant, V_0 is the peak voltage when the first stage of the loading process ends. Let $t = T_o$ and substituting Eq. (1′) into Eq. (1) yields

$$V_o = K \cdot F_o \cdot e^{-\left(\frac{T_o}{\tau_d}\right)^{\beta}} \tag{2′}$$

Eq. (2) represents that the piezovoltage decays in a typical exponential law. The fitted functions for the piezovoltage of sample 1 are, then, written as

$$V(t) = \begin{cases} -0.271F_o \frac{t}{T_o} e^{-\left(\frac{t}{11.79}\right)^{0.2993}} & (t \leqslant T_o) \\ -0.271F_o e^{-\left(\frac{T_o}{11.79}\right)^{0.2993}} \cdot e^{-\left(\frac{t}{94}\right)} & (t > T_o) \end{cases} \tag{3}$$

In Fig. 4 (a)–(e) the red curves represent the fitting function (3) with different F_o and T_o and the blue curves are the corresponding measured piezovoltages. Fig. 4(a)–(c) shows three fitting curves with F_o = 150 N and T_o = 250, 500, 1000 ms, respectively. Fig. 4(d) and (e) shows two fitting curves with T_o = 250 ms and F_o = 50, 100 N, respectively. It is evident that the fitted functions coincide well with the measured curves. The values of K, τ_d, β and τ_c, are listed in Table 2.

The fitted functions for sample 2 are as following

$$V(t) = \begin{cases} -0.295F_o \frac{t}{T_o} e^{-\left(\frac{t}{12.74}\right)^{0.302}} & (t \leqslant T_o) \\ -0.295F_o e^{-\left(\frac{T_o}{12.74}\right)^{0.302}} \cdot e^{-\left(\frac{t}{93}\right)} & (t > T_o) \end{cases} \tag{4}$$

Again, in Fig. 5(a)–(f) the red curves represent the fitting function (4) with different F_o and T_o and the blue curves are the corresponding measured piezovoltages. Fig. 5 (a)–(c) shows three fitting curves with F_o = 150 N and T_o = 250, 500, 1000 ms, respectively, while Fig. 5(d)–(f) shows the same three measured curves but corresponding to the unloading portion, in which the red curves are obtained using the same fitting functions as those in Fig. 5(a)–(c). The coincidence of the curves in Fig. 5(d)–(f) imply that the piezovoltage curves during unloading process have the similar waveforms as those in loading process.

It was found that all the piezovoltage curves of the six samples have the same form of fitting function. The first part (stretched exponential term) of the fitting function is characterized by three parameters: the proportional coefficient K, stretching exponent β, and time constant τ_d. While the second part (typical exponential term) is characterized only by one parameter: time constant τ_c, which is easy to be determined. These parameters are independent of holding load F_o and loading time T_o. To determine the three parameters in the first part at least five piezovoltage–time curves are measured for each sample corresponding to different holding load F_o and loading time T_o, as shown in Fig. 4. We obtained the three parameters by fitting any three of the five curves to Eq. (1) using trial-and-error method on a computer. Then the other two curves were fitted by the three determined parameters, with corresponding values of F_o and T_o, for checking the adequacy of fitting. It was found that once the three parameters were determined by any three curves, they are available for the remaining two curves. This proved the uniqueness of the fitting. Namely, the stretched exponential behavior represents merely bone's inherent property. The fitting parameters of the six samples are listed in Table 2.

Table 2
Fitting parameters.

Sample no.	Fitting parameters			
	β	K	τ_d (ms)	τ_c (ms)
1	0.299	−0.272	11.79	94
2	0.302	−0.295	12.74	93
3	0.305	−0.212	10.98	60
4	0.276	−0.190	11.44	115
5	0.286	−0.214	9.30	81
6	0.291	−0.213	11.42	88
Mean ± SD	0.293 ± 0.01	−0.233 ± 0.038	11.28 ± 1.037	88.5 ± 16.4

The time constant τ_d, in loading process, is about one order of magnitude smaller than the τ_c, in loading hold process. The significance of the stretched exponent β($0.276 < \beta < 0.305$) is that the relaxation mechanism in loading process is different from that in load holding process. The fitting functions (3) and (4) and the measured piezovoltage curves in Figs. 4 and 5 show that the peaks of piezovoltage are proportional to the maximum load F_o and inversely proportional to loading interval T_o. Making use of the mean value of the fitting parameters listed in Table 1, the fitting function (1) of the bone can be further written as

$$V(t) = \begin{cases} -0.233F_o \frac{t}{T_o} e^{-\left(\frac{t}{11.28}\right)^{0.293}} & (t \leqslant T_o) \\ -0.233F_o e^{-\left(\frac{T_o}{11.28}\right)^{0.293}} \cdot e^{-\left(\frac{t}{88.5}\right)} & (t > T_o) \end{cases}$$

4. Discussion

Although the stretched exponential law is an empirical function (Williams and Watts, 1970; Kawakami and Pikal, 2005; Milovanov et al., 2008), it has been found that the function can describe the relaxation behavior of a variety of materials with structural disorder such as dielectrics (Milovanov et al., 2008, 2007; Husain and Anderssen, 2005; Fu et al., 2001), amorphous substances like glasses (Haruyama et al., 2007; Palmer et al., 1984), and soft tissues (June et al., 2009; MacLean et al., 2007). A natural and commonly used interpretation of an observed stretched exponential relaxation is in terms of the global relaxation of a system containing many independently relaxing species, each of which decays exponentially in time with a specific fixed relaxation rate (Johnston, 2006). Further, the stretched exponential relaxation can be expressed as a weighted superposition of single exponential relaxation functions (Milovanov et al., 2008, 2007; Palmer et al., 1984; Johnston, 2006; Richert and Richert, 1998)

$$e^{-\left(\frac{t}{\tau_d}\right)^{\beta}} = \int_0^{\infty} p(\tau,\beta) e^{-\left(\frac{t}{\tau}\right)} d\tau$$

where $p(\tau,\beta)$ is the weighting function, which can be expressed in terms of a stable distribution of various individual relaxation with different time constant τ. Then τ_d is a constant which represents a global effect of the large number of different relaxation time constants, and it is sometime also known as apparent time constant.

Actually, relaxations of the piezovoltage imply that the piezoelectric charges on the electrodes mainly discharge through the impedance of bone between the two electrodes. Because the input impedance of Head Stage is at least two orders higher than the impedance of bone between the two electrodes, it can be considered that the piezoelectric charges mainly discharge through the bone impedance. Singh and Saha, and Johnson described the electrical behavior of bone in terms of an equivalent parallel combination of impedance and capacitor (Singh and Saha, 1984; Johnson et al., 1980). Its capacitance is $C = \varepsilon S/d$ (parallel plate capacitors) where ε stands for the dielectric constant of bone between the two electrodes, S denotes area of the electrode, and d represents thickness of the bone sample. Therefore, the factors influence the discharge behavior should be merely two electric properties of bone: the capacitance and impedance or resistance. The resistance of the bone between the two electrodes is approximately $R = \rho d/S$ where ρ denotes bone's resistivity. The resistance R and capacitance C form a parallel connected RC circuit. The time constant τ_c can, then, be defined as $\tau_c = RC = \varepsilon\rho$, which means that the discharge rate of piezocharges on the electrodes depends on dielectric constant ε and resistivity ρ.

In load holding process, τ_c is approximately a constant and hence the voltage relaxation follows a typical exponential decay. In loading or unloading process, however, the voltage relaxation shows multi-relaxation time behavior. A possible explanation is that, during the duration of deformation, the bone's dielectric or the resistivity properties varies, which leads to changes of relaxation behavior. Because the piezoelectricity of bone arises from the organic components (mainly collagen), the analysis mainly focuses on the collagen fiber structure. The structural details are shown in Fig. 6 (Minary-Jolandan and Yu, 2009; Jager and Fratzl, 2000; Fratzl and Weinkamer, 2007; Gupta et al., 2006). A collagen molecule is composed of a triplet of three polypeptide chains (two α_1 and one $\alpha_2$chains) with length about 300 nm, and diameter about 1.5 nm (Fig. 6(a)). These molecules lie in a staggered arrangement, and there is a 40 nm gap between one collagen molecule end and another. The adjacent collagen molecules are joined by covalent cross-links near the gaps. Collagen molecules are filled and coated by platelet like tiny mineral crystals, which form the mineralized collagen fibril. A group of collagen fibrils embedded in the mineral crystals form a hierarchical structure of collagen fiber (Fig. 6(b)).

When the bone is stressed, the mineral platelet transfers the stress via adjacent collagen fibrils and cross links by shearing, and the shear deformations of the organic fibrils are considerably larger than the mineralized components (Gupta et al., 2006).

The triple helices structure and the considerably large deformation may well be the two main factors influencing the electric properties of bone tissues during the deformation. During the loading or unloading process, it was probable that the large deformation included self-deformations of the three collagen molecule chains leading to piezo-polarization and continuous relative slipping movement between the chains. However, in load holding process, the slipping movements stopped. A hypothesis is then made that the slipping movements between adjacent chains may cause the variations of the electric properties of collagens, which includes either the dielectric constant or the resistivity or both of them ($\varepsilon\rho$). If the hypothesis holds true for collagen materials, it may be considered that variation of electric properties of bone is associated with geometrical distribution of collagen fibrils. If the above analysis holds true for collagen materials, it may be considered that variation of electric properties of bone is associated with geometrical distribution of collagen fibrils. Because the collagen fibrils orient randomly in various directions in bone, with the mean direction approximately parallel to the axis of bone diaphysis (Ascenzi and Lomovtsev, 2006; Bills et al., 1982), the variation extent of electric properties of collagen fibers may depend on their orientation angles. In other words, the changes of the electric properties are different for the collagen fibers with different directions. Thus, the collagen fibrils possessed multi-relaxation behaviour, while in load holding process, there is no continuous slipping movement between chains, and they recover to typical exponential behavior. One of the two results of variation in the dielectric properties of bone was the change of equivalent capacitance ($C = \varepsilon S/d$) between the electrodes. An increase in the dielectric constant ε leads to an increase in the capacitance and then the piezovoltage between the electrodes becomes lower, with the piezocharges stored in C remaining the same, and vice versa. The other result is the variation of the resistivity or resistance of bone which affecting the piezovoltages by changing the charge/discharge rate.

The curves in Fig. 7 illustrate the decay characteristics of the stretching and typical exponential laws. Fig. 7 shows four curves for the decay exponential function $e(t) = e^{-(t/\tau)^{\beta}}$. The Blue and Green ones are the typical exponential relaxation curves ($\beta = 1$) with $\tau = 60$ and 88.5 ms which corresponds to the smallest and average time constants τ_c, respectively, as shown in Table 2. The Red and Black one are stretched exponential relaxation curves with $\tau = 12.74$ ms, $\beta = 0.302$ and $\tau = 9.30$ ms, $\beta = 0.286$ (the largest and smallest time constant τ_d, see also Table 2). These curves indicate that the stretched exponential curves decay faster than the typical exponential curves at and before approximately 120 (Red) or 220 (Black) ms and beyond that they decay slower than the typical exponential curves.

It is evident from the four simulative relaxation curves in Fig. 7 that the electric properties of bone are changed during the deformation process. The first two (Blue and Green) and the last two (Red and Black) curves simulate, respectively, the piezovoltage relaxation characteristics without and with changes of the dielectric constants, which are equivalent to change in the capacitance. Because once the dielectric constant or capacitance increases, the piezovoltage across the capacitor becomes lower. This trend is in agreement with the Red and Black curves in Fig. 7 for the whole duration. It is also noted that if the resistivity keeps unchanged or increases, the equivalent relaxation time constant must increase as predicted above. Then the overall decay becomes slower. In reality, even the resistivity becomes lower, the product of $\varepsilon\rho$ is still likely to increase, which making the relaxation rate slowly. Besides the piezoelectricity, the other mechanism of SGPs is the streaming potential in bone. The relaxation of the streaming potentials in living bone, caused by step-load, also follows a stretched exponential decay (Qin et al., 2002). It is possible that a certain correlation exists between the piezoelectricity and the steaming potentials in bone.

Generally, during the deformation of bone the viscoelastic deformation such as creep may also occur though the creep deformation is relative small in dry cortical bone (Yamashita et al., 2002). However, if this kind of deformation is indeed big enough to influences the variations of the electric properties of collagens to a certain extent, it would cause the variations of the electric properties during both loading and load holding processes, and thus the difference of the two kinds of relaxation modes,

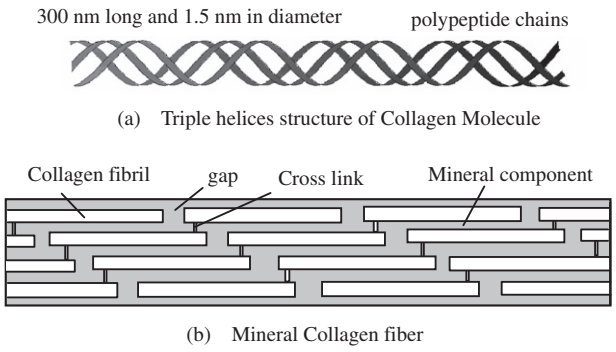

Fig. 6. Schematic illustration of mineral collagen fiber and triple helices structure of molecule.

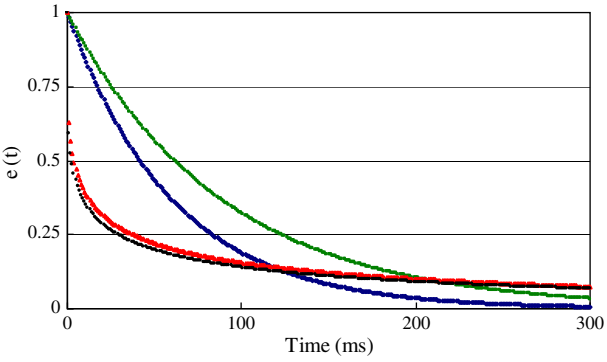

Fig. 7. Curves for the decay exponential function.

corresponding to loading and load holding processes respectively, will not occur. Based on this judgment, the creep does not influence the relaxation behavior.

5. Conclusions

The pizeovoltage of bone show different relaxation behaviors in loading and load holding processes. In loading process, the piezovoltage decay follows a stretched exponential law, while it follows the typical exponential law in load holding process. The stretched exponential behavior is independent of loading amplitude and rate. The apparent time constants of the stretched exponential are approximately one order of magnitude smaller than the time constants of typical exponential law.

To explain the observations, a hypothesis was proposed that the slipping movements between adjacent collage molecules cause the variations of the electric properties of collagens. Based on the hypothesis the deduced main reason for the stretching-exponential behavior is the triple helices structure of collagen fibrils distributed randomly in bone, which suffer relatively large deformation, under external loads, including self-deformations and relative slipping between molecule chains. The relative slipping movements may change the dielectric constants and resistances of bone, which leads to multiple relaxation time behaviors during deformation of bone.

Acknowledgment

The work was supported by the National Natural Science Foundation of China under Grant No. 10672119.

Appendix A. The fitting scheme for stretched exponential function

Substituting Eq. (1′) into Eq. (1), we have

$$V(t) = KF_0 \frac{t}{T_o}(t) e^{-\left(\frac{t}{\tau_d}\right)^{\beta}} \quad t \leqslant T_0 \tag{a}$$

As there are three unknown parameters K, τ_d and β in Eq. (a), three measured piezovoltage–time curves, at different load magnitude F_o and loading time T_o, of each sample are employed to determine them.

For the convenience of calculation, without loss of generality, the measured piezovoltage–time curves, denoted as $\overline{V}(t)$, at loading time $T_o = 0.25$, 0.5, 1 s, respectively, and load magnitude $F_o = 100$ N were used in the fitting calculation. For simplicity, denote the loading time $T_o = 0.25$, 0.5, 1 s and the corresponding three measured piezovoltages as T_{025}, T_{05}, T_1 and $\overline{V}_{025}(t)$, $\overline{V}_{05}(t)$, $\overline{V}_1(t)$, respectively. Further, the time t in $\overline{V}_{025}(t)$, $\overline{V}_{05}(t)$, $\overline{V}_1(t)$ is denoted as t_{025}, t_{05} and t_1, respectively Substituting the three piezovoltages into Eq. (a), respectively, following three equations are obtained

$$\overline{V}_{025}(t_{025}) = KF_0 \frac{t_{025}}{T_{025}} e^{-\left(\frac{t_{025}}{\tau_d}\right)^{\beta}} \quad t_{025} \leqslant T_{025} \tag{b}$$

$$\overline{V}_{05}(t_{05}) = KF_0 \frac{t_{05}}{T_{05}} e^{-\left(\frac{t_{05}}{\tau_d}\right)^{\beta}} \quad t_{05} \leqslant T_{05} \tag{c}$$

$$\overline{V}_1(t_1) = KF_0 \frac{t_1}{T_1} e^{-\left(\frac{t_1}{\tau_d}\right)^{\beta}} \quad t_1 \leqslant T_1 \tag{d}$$

The ratio of Eq. (b) to Eq. (c) yields

$$\frac{\overline{V}_{025}(t_{025})}{\overline{V}_{05}(t_{05})} = \frac{T_{05}t_{025}}{T_{025}t_{05}} e^{(\frac{t_{05}}{\tau_d})^{\beta} - (\frac{t_{025}}{\tau_d})^{\beta}}$$

Applying the logarithm to the equation above, we have

$$\ln\left[\frac{\overline{V}_{025}(t_{025})}{\overline{V}_{05}(t_{05})}\frac{T_{025}t_{05}}{T_{05}t_{025}}\right] = \frac{t_{05}^{\beta} - t_{025}^{\beta}}{\tau_d^{\beta}}$$

Thus, the time constant τ_d equals to

$$\tau_d = \left\{\frac{t_{05}^{\beta} - t_{025}^{\beta}}{\ln\left[\frac{\overline{V}_{025}(t_{025})}{\overline{V}_{05}(t_{05})}\frac{T_{025}t_{05}}{T_{05}t_{025}}\right]}\right\}^{\frac{1}{\beta}} \tag{e}$$

By Eq. (a), the proportional coefficient K is

$$K = \frac{\overline{V}_{025}(t_{025})}{F_0 \frac{t_{025}}{T_{025}} e^{-\left(\frac{t_{025}}{\tau_d}\right)^{\beta}}} \tag{f}$$

It is clear that once the stretching exponent β is known, τ_d and K are obtained. Moreover, similar equations to Eqs. (e) and (f) can be obtained from the ratios of the other equations. In order to distinguish the parameters calculated from other ratios, the τ_d and K in the equations above is replaced by τ_{d12} and k_{12}. Thus, Eqs. (e) and (f) can be rewritten as

$$\tau_{d12} = \left\{\frac{t_{05}^{\beta} - t_{025}^{\beta}}{\ln\left[\frac{\overline{V}_{025}(t_{025})}{\overline{V}_{05}(t_{05})}\frac{T_{025}t_{05}}{T_{05}t_{025}}\right]}\right\}^{\frac{1}{\beta}} \tag{g-1}$$

$$k_{12} = \frac{\overline{V}_{025}(t_{025})}{F_0 \frac{t_{025}}{T_{025}} e^{-\left(\frac{t_{025}}{\tau_{d12}}\right)^{\beta}}} \tag{g-2}$$

Similarly, τ_{d23}, k_{23}, τ_{d31} and k_{31} can be defined similarly:

$$\tau_{d23} = \left\{\frac{t_1^{\beta} - t_{05}^{\beta}}{\ln\left[\frac{\overline{V}_{05}(t_{05})}{\overline{V}_1(t_1)}\frac{T_{05}t_1}{T_1t_{05}}\right]}\right\}^{\frac{1}{\beta}} \tag{h-1}$$

$$k_{23} = \frac{\overline{V}_{05}(t_{05})}{F_0 \frac{t_{05}}{T_{05}} e^{-\left(\frac{t_{05}}{\tau_{d23}}\right)^{\beta}}} \tag{h-2}$$

$$\tau_{d31} = \left\{\frac{t_{025}^{\beta} - t_1^{\beta}}{\ln\left[\frac{\overline{V}_1(t_1)}{\overline{V}_{025}(t_{025})}\frac{T_1t_{025}}{T_{025}t_1}\right]}\right\}^{\frac{1}{\beta}} \tag{i-1}$$

$$k_{31} = \frac{\overline{V}_1(t_1)}{F_0 \frac{t_1}{T_1} e^{-\left(\frac{t_1}{\tau_{d_1}}\right)^{\beta}}} \tag{i-2}$$

The ideal fitting result is to find a specific value of β, which makes $\tau_d = \tau_{d12} = \tau_{d23} = \tau_{d31}$ and $K = k_{12} = k_{23} = k_{31}$.

Due to the presence of measurement errors, the fitting criterion used is to find a β ($0 < \beta < 1$) which makes the error function

$$Error = (|\tau_{d12} - \tau_{d23}| + |\tau_{d23} - \tau_{d31}| + |\tau_{d31} - \tau_{d12}|) \times (|k_{12} - k_{23}| + |k_{23} - k_{31}| + |k_{31} - k_{12}|)$$

minimum under the six restrictive conditions $|\tau_{d12} - \tau_{d23}| \leqslant \Delta\tau$, $|\tau_{d23} - \tau_{d31}| \leqslant \Delta\tau$, $|\tau_{d31} - \tau_{d12}| \leqslant \Delta\tau$, $|k_{12} - k_{23}| \leqslant \Delta k$, $|k_{23} - k_{31}| \leqslant \Delta k$ and $|k_{31} - k_{12}| \leqslant \Delta k$, which $\Delta\tau$ and Δk are error threshold of time constants and proportional coefficients, respectively. Then the values of τ_d and k are defined as their average $\tau_d = (\tau_{d12} + \tau_{d23} + \tau_{d31})/3$ and $K = (k_{12} + k_{23} + k_{31})/3$. Because τ_d and K are not of the same order of magnitude, the error function is configured by multiplying the sum of three time constant differences and the sum of the three proportional coefficient differences.

The Eqs. (g-1), (g-2), (h-1), (h-2), (i-1) and (i-2) imply that if a specific β is found K, τ_d can be determined based on the three pizeovoltage values of $\overline{V}_{025}(t_{025})$, $\overline{V}_{05}(t_{05})$ and $\overline{V}_1(t_1)$ at specific time t.

For the performance of the curve fitting, the three pizeovoltage of $\overline{V}_{025}(t_{025})$, $\overline{V}_{05}(t_{05})$ and $\overline{V}_1(t_1)$ at $t_{025} = 0.25$ s, $t_{05} = 0.5$ s and $t_1 = 1$ s, respectively, were used, which corresponding to the three peak values of the three pizeovoltage–time curves.

In order to find suitable fitting results under the above criterion, circular calculations were carried out for the above equations when β increases from 0 to 1 step by step. The obtained parameters K, τ_d and β were listed in Table 2 in the text.

It was found that if the value of $\Delta\tau$ or Δk is set to be less than 5–8% of the final fitting value of τ_d or K, the fitting calculation cannot reach convergent results due to the presence of measurement errors. Thus we use 10% of final fitting values of the two parameters as the tolerance in the calculations, which means that the relative difference of the final fitting value with respect to each of the calculation value (such as $\Delta\tau$ with respect to τ_{d12} or τ_{d23} or τ_{d31}) is below 10%.

References

Anderson, J.C., Eriksson, C., 1968. Electrical properties of wet collagen. Nature 218, 166–168.

Ascenzi, M.G., Lomovtsev, A., 2006. Collagen orientation patterns in human secondary osteons, quantified in the radial direction by confocal microscopy. J. Struct. Biol. 153, 14–30.

Aschero, G. et al., 1999. Statistical characterization of piezoelectric coefficient d_{23} in cow bone. J. Biomech. 32, 573–577.

Bassett, C.A.L., Becker, R.O., 1962. Generation of electric potentials by bone in response to mechanical stress. Science 137, 1063–1064.

Bills, P.M. et al., 1982. Mineral-collagen orientation relationships in bone. J. Chem. Crystallogr. 12, 51–63.

Burger, E.H. et al., 2003. Strain-derived canalicular fluid flow regulates osteoclast activity in a remodelling osteon-a proposal. J. Biomech. 36, 1453–1459.

Fondrk, M. et al., 1988. Some viscoplastic characteristics of bovine and human cortical bone. J. Biomech. 21, 623–630.

Fratzl, P., Weinkamer, R., 2007. Nature's hierarchical materials. Prog. Mater. Sci. 52, 1263–1334.

Fu, D.H. et al., 2001. Observation of piezoelectric relaxation in ferroelectric thin films by continuous charge integration. Jpn. J. Appl. Phys. 40, 5683–5686.

Fu, D.H. et al., 2006. Analysis of the waveforms of piezoelectric voltage of bone. J. Tianjin. Univ. Sci. Tech. 39, 349–353.

Fukada, E., 1964. Piezoelectic effects in collagen. Jpn. J. Appl. Phys. 3, 117–121.

Gupta, H.S. et al., 2006. Cooperative deformation of mineral and collagen in bone at the nanoscale. PNAS 103, 17741–17746.

Haruyama, O. et al., 2007. The free volume kinetics during structural relaxation in bulk Pd-P based metallic glasses. Mater. Sci. Eng. A, 497–500.

Hoc, T. et al., 2006. Effect of microstructure on the mechanical properties of Haversian cortical bone. Bone 38, 466–474.

Husain, S.A., Anderssen, R.S., 2005. Modelling the relaxation modulus of linear viscoelasticity using Kohlrausch functions. J. Non-Newtonian Fluid. Mech. 125, 159–170.

Jager, I., Fratzl, P., 2000. Mineralized collagen fibrils: a mechanical model with a staggered arrangement of mineral particles. Biophys. J. 79, 1737–1746.

Johnson, W.M. et al., 1980. Comparison of the electromechanical effects in wet and dry bone. J. Biomech. 13, 437–442.

Johnston, D.C., 2006. Stretched exponential relaxation arising from a continuous sum of exponential decays. Phys. Rev. B 74, 184430.

June, R.K. et al., 2009. Cartilage stress-relaxation is affected by both the charge concentration and valence of solution cations. Osteoarthr. Cartil. 17, 669–676.

Kalinin, S.V. et al., 2005. Electromechanical imaging of biological systems with sub-10 nm resolution. Appl. Phys. Lett. 87, 053901.

Kawakami, K., Pikal, M.J., 2005. Calorimetric investigation of the structural relaxation of amorphous materials: evaluating validity of the methodologies. J. Pharm. Sci. 94, 948–965.

MacLean, J.J. et al., 2007. Role of endplates in contributing to compression behaviors of motion segments and intervertebral discs. J. Biomech. 40, 55–63.

Milovanov, A.V. et al., 2007. Stretched exponential relaxation and ac universality in disordered dielectrics. Phys. Rev. B 76, 104201.

Milovanov, A.V. et al., 2008. Stretched-exponential decay functions from a self-consistent model of dielectric relaxation. Phys. Lett. A 372, 2148–2154.

Minary-Jolandan, M., Yu, M.F., 2009. Nanoscale characterization of isolated individual type I collagen fibrils: polarization and piezoelectricity. Nanotechnology 20, 085706.

Palmer, R.G. et al., 1984. Models of hierarchically constrained dynamics for glassy relaxation. Phys. Rev. Lett. 53, 958–961.

Pienkowski, D., Pollack, S.R., 1983. The origin of stress-generated potentials in fluid-saturated bone. J. Orthop. Res. 1, 30–41.

Qin, Q.H., 2001. Fracture Mechanics of Piezoelectric Materials. WIT Press, Southampton.

Qin, Q.H., Ye, J.Q., 2004. Thermolectroelastic solutions for internal bone remodeling under axial and transverse loads. Int. J. Solids Struct. 41, 2447–2460.

Qin, Q.H. et al., 2005. Thermolectroelastic solutions for surface bone remodeling under axial and transverse loads. Biomaterials 26, 6798–6810.

Qin, Y.X. et al., 2002. The pathway of bone fluid flow as defined by in vivo intramedullary pressure and streaming potential measurements. Ann. Biomed. Eng. 3, 693–702.

Richert, R., Richert, M., 1998. Dynamic heterogeneity, spatially distributed stretched-exponential patterns, and transient dispersions in solvation dynamics. Phys. Rev. E 58, 779–784.

Riddle, R.C., Donahue, H.J., 2008. From streaming potentials to shear stress: 25 years of bone cell mechanotransduction. J. Orthop. Res. 27, 143–149.

Singh, S., Saha, S., 1984. Electrical properties of bone: a review. Clin. Orthop. Relat. Res. 186, 249–271.

Steinberg, M.E. et al., 1968. Electrical potentials in stressed bone. Clin. Orthop. Relat. Res. 61, 294–300.

Tzima, E. et al., 2005. A mechanosensory complex that mediates the endothelial cell response to fluid shear stress. Nature 437, 426–431.

Tzukert, A. et al., 1983. Electroconductivity of bone in vitro and in vivo. Clin. Orthop. Relat. Res. 179, 270–274.

Williams, G., Watts, D.C., 1970. Non-symmetrical dielectric relaxation behavior arising from a simple empirical decay function. Trans. Faraday Soc. 66, 80–85.

Yamashita, J. et al., 2002. Collagen and bone viscoelasticity: a dynamic mechanical analysis. J. Biomed. Mater. Res. 63, 31–36.

Yokota, H., Tanaka, S.M., 2005. Osteogenic potentials with joint-loading modality. J. Bone Mineral Metabol. 23, 302–308.